Carbohydrate Polymers 93 (2013) 574–581

Contents lists available at SciVerse ScienceDirect

Carbohydrate Polymers

journal homepage: www.elsevier.com/locate/carbpol

Self-association of novel mixed 3-mono-*O*-alkyl cellulose: Effect of the hydrophobic moieties ratio

Antonio Sullo[a,*], Yunhui Wang[b], Andreas Koschella[b], Thomas Heinze[b], Tim J. Foster[a]

[a] University of Nottingham, Division of Food Sciences, School of Biosciences, Sutton Bonington Campus, Loughborough LE12 5RD, United Kingdom
[b] Friedrich Schiller University of Jena, Institute for Organic Chemistry and Macromolecular Chemistry, Center of Excellence for Polysaccharide Research, Humboldtstraße 10, D-07743 Jena, Germany

ARTICLE INFO

Article history:
Received 14 August 2012
Received in revised form
12 November 2012
Accepted 15 November 2012
Available online 20 December 2012

Keywords:
Hydrophobic biopolymer
Functionalization of polysaccharides
Rheology
3-*O*-alkyl cellulose
Differential scanning calorimetry
Self-association
Regioselectively substituted cellulose
Two-state model
Regioselective cellulose

ABSTRACT

Heat-induced self-association of regioselectively functionalized 3-*O*-alkyl celluloses bearing both ethyl- and propyl groups dissolved in water was studied by means of differential scanning calorimetry and oscillatory shear rheology. The measured degrees of substitution were close to 1 but the ratio of ethyl (DS_{Et}) to propyl groups (DS_{Pr}) was varied. The aggregation process is intimately coupled with phase separation as shown by the appearance of clouding in the same temperature range. Phase separation is arrested by the incipient gelation; whereby "stronger" gels are produced with high amounts of the propyl substituent than "weaker" phase separating samples as the amount of ethyl groups increases and the amount of propyl groups decreases. The correlation between rheology and thermal analysis clearly demonstrates that aggregation leads to formation of a gel network. It was found that as the ethyl moiety is replaced by propyl group the enthalpies of the thermal transitions increase strongly together with an increase of the elastic modulus (G') and the network is also more coherent with a steady decrease in $\tan\delta$ (G''/G'). Reversibility was observed on cooling with a marked hysteresis for samples containing high levels of propyl groups. Hysteresis on cooling was explained in term of additional consolidation of the structure occurring at temperature much higher than the aggregation temperature, possibly involving backbone–backbone interactions. Quantitative analysis of the DSC data, based on the two-state thermodynamic model described by Armstrong et al. (1995) enabled evaluation of the van't Hoff enthalpy and the aggregation number. On the basis of those thermodynamic parameters, an "intermolecularly bridged clusters" model is proposed for the heat-induced transition of 3-*O*-ethyl-propyl cellulose ethers. The van't Hoff enthalpy/calorimetric enthalpy ratio $\Delta H_{vH}/\Delta H_{cal}$ further indicates on the cooperativity of the process. The number of clusters and indeed the number of molecular chains comprising a cluster are both dependent upon the ratio of the two hydrophobic moieties. An increase in the aggregation number (n) (more aggregates coming together) occurs as ethyl is replaced by propyl, consistent with the observation of a "stronger" gel. The effect of the two different moieties on the physico-chemical properties of 3-*O*-ethyl-propyl cellulose ethers has been explained in term of different size/hydrophobicity of the two moieties and their distribution.

1. Introduction

Functionalization of natural organic molecules, such as polysaccharides, embodies a promising starting point for the synthesis of well defined supramolecular structures, held together by relatively weak non-covalent interactions, with interesting rheological properties. In this context, hydrophobically modified celluloses ethers are water-soluble polymers which are made of hydrophobic groups chemically attached to a hydrophilic polysaccharide backbone. The accessible reactive hydroxyl groups for substitution are at the *C*-2, *C*-3, and *C*-6 atoms of the glucose unit (Heinze & Petzold, 2008, chap. 16; Koschella, Fenn, Illy, & Heinze, 2006). An important property of cellulose ethers is their ability to self-associate in aqueous solution, when the temperature increases above a certain critical value, in which they have found wide application as thermo-responsive polymer (Ganz, 1977; Grover, 1993). The presence of the hydrophobic group on the cellulose backbones has important implications for the behaviour of cellulose ethers in water, which is primarily a consequence of changes in the surrounding water rather than water–solute interactions (Tanford, 1978; Israelachvili & Pashley, 1982; Wiggins, 1997; Yaminsky and Erwin (2001)). Structuring of

Abbreviations: PR, 3-*O*-ethyl-propyl cellulose ethers; DS, degree of substitution; DS_{Et}, DS of ethyl groups; DS_{Pr}, DS of propyl groups; DSC, differential scanning calorimetry; G', elastic modulus; G'', loss modulus.

* Corresponding author. Tel.: +44 0 115 951 6246; fax: +44 0 115 951 6020.
E-mail address: tim.foster@nottingham.ac.uk (A. Sullo).

0144-8617/$ – see front matter © 2012 Elsevier Ltd. All rights reserved.
http://dx.doi.org/10.1016/j.carbpol.2012.11.093

water molecules (ice-like) and the entropy penalty carried with it have been often employed to explain the aggregation of hydrophobic solutes in water (hydrophobic effect) (Tanford, 1978; Wiggins, 1997). A phenomenon, concomitant to aggregation, is phase separation, observed visually as an increase in turbidity of the solution (Sarkar & Walker, 1995). Phase diagrams of cellulose ethers in water show the characteristic low critical solution temperature, above which the system undergoes phase separation (Chevillard & Axelos, 1997; Hirrien, Chevillard, Desbrières, Axelos, & Rinaudo, 1998; Robitaille, Turcotte, Fortin, & Charlet, 1991). At appreciable concentration those aggregates develop in to a coherent gel (thermogelation) which reverses back to a solution on a subsequent cooling (Heymann, 1935). Thermogelation parameters such as temperature of gelation (T_{gel}). entropy of aggregation and gel elasticity are mainly controlled by: nature of the substituents, degree of substitution (DS) and substitution pattern along the cellulose chain (Desbrieres, Hirrien, & Rinaudo, 1998; Haque, Richardson, Morris, Gidley, & Caswell, 1993; Hirrien, Desbrières, & Rinaudo, 1996; Nishinari, Hofmann, Moritaka, Kohyama, & Nishinari, 1997; Sarkar, 1995; Sun et al., 2009). For instance, a random distribution of the alkyl groups along the backbone is responsible for presence of residual crystallinity which causes the chains to be dispersed in bundles, at low temperatures, as proposed by Haque and Morris (1993). During the initial stages of heating the bundles gradually open. On further heating, the disruption of the water cages will cause polymer–polymer hydrophobic association to form a percolating network, evidenced by a multi-technique approach to measurement of the system (Funami et al., 2007; Haque & Morris, 1993; Haque et al., 1993; Li et al., 2001; Li, 2002; Sarkar, 1979). Within the substituted region along the polymer chain glucose units could have all three of their available hydroxyl groups substituted, or only one or two, and the presence of three-methyl substituted glucose is necessary for the gelation to occur (Hirrien et al., 1998). There is still a certain degree of controversy regarding the mechanism of gelation whereby other authors have emphasized the role of the concomitant phase separation (Desbrières, Hirrien, & Ross-Murphy, 2000; Ibbett, Philp, & Price, 1992; Kobayashi, Huang, & Lodge, 1999). The different mechanisms all involve interaction between the hydrophobic moieties on the cellulose backbones (Kato, Yokoyama, & Takahashi, 1978). Discrepancy in the interpretation of the mechanism of thermogelation also owes to the lack of model polymer with a precise distribution of the substituent, in contrast to their synthetic equivalents. Recent advances in synthetic pathways has opened to the possibility of substituting the whole cellulose chain regioselectively, i.e. exclusively at positions 2, 3 or 6 (Fox, Li, Xu, & Edgar, 2011; Heinze & Petzold, 2008, chap. 16; Koschella et al., 2006). A comparative study on the thermo-rheological properties between regioselectively substituted 3-*O*-ethylcellulose and its randomly substituted equivalent has shown substantial difference in the thermo-rheological properties (Sun et al., 2009). The temperature of the sol–gel transition is much lower for the randomly substituted cellulose (30 °C) than for the regioselectively substituted cellulose equivalent (60 °C). Moreover the gel formed was much weaker than the random counterpart. The regioselectively substituted cellulose reversed back to the solution state on cooling giving rise to two distinct exothermic events, as observed in the calorimeter, opposed to a single event observed for randomly substituted cellulose ethers. The explanation for the two events on cooling was based on the Haque and Morris (1993) model. It was suggested that the ethyl substitution does not eliminate completely the crystalline structure of the native cellulose since there are still two positions (2 and 6) available for hydrogen bonding in agreement with the work of Kondo, Koschella, Heublein, Klemm, and Heinze (2008). However the reconstitution of the original structures in solution, on cooling, is more difficult due to the regular allocation of the substituents onto the cellulose backbones, which give rise to the lower temperature event. It was also reported that the size of the hydrophobic substitute changes the solubility–temperature relationship of these polymers. Heinze, Pfeifer, Sarbova, and Koschella (2011) reports about 3-*O*-propyl cellulose ether with a very low flocculation temperature, whereas 3-*O*-buytyl cellulose is insoluble in water. It appears that when cellulose derivatives are composed of a homogeneous chemical structure, their physicochemical properties may be directly predicted which has incredible advantages. As a continuation of the Sun et al. (2009) work, the thermogelation properties of new regioselective cellulose ethers, with varying ratios of ethyl to propyl substituents, were studied by coupling rheological with thermal measurements. The purpose of this specific substitution was to investigate the possibility of tuning physico-mechanical properties of those materials by either controlling the length of the alkyl moiety and/or the ratio of ethyl and *n*-propyl groups.

Table 1
Composition of 3-*O*-alkyl celluloses bearing two different alkyl groups at position 3.

Sample	DS_{total}	DS_{Et}/DS_{Pr}	DS_{Et}	DS_{Pr}	M_n[a] (g/mol)
$H_{Et/Pr}$	1.10	6.33	0.95	0.15	45,917
$M_{Et/Pr}$	1.04	2.85	0.77	0.27	49,276
$L_{Et/Pr}$	0.83	0.48	0.27	0.56	33,308
Pr	1.09	0	0	1.09	n.a.

[a] Number average molar mass measured by SEC.

2. Materials and methods

2.1. Mixed 3-mono-O-alkyl cellulose

3-Mono-*O*-alkyl cellulose was synthesized using two different alkyl agents, ethyl and/or propyl, in four different molar ratios, via 2,6-di-*O*-thexyldimethylsilyl cellulose (Heinze, Wang, Koschella, Sullo, & Foster, 2012). The degree of substitution (DS) for the four samples studied was determined by ^{1}H NMR spectroscopy of the peracetylated samples (Table 1), a complete description of the structural properties of these samples can be found elsewhere (Heinze et al., 2012). Samples are named based on the abbreviation reported in Table 1. "Pr" indicates 3-*O*-propyl cellulose while "$L_{Et/Pr}$ and $H_{Et/Pr}$" indicates 3-*O*-ethyl propyl cellulose with respectively low, medium or high ratio of the two hydrophobic moieties (DS_{Et}/DS_{Pr}).

2.2. Solution preparation

Regioselective cellulose derivatives were dissolved in distilled water at temperature close to 2 °C using an ice water bath. Dissolution was achieved after 24 h with continuous stirring. Solutions were then centrifuged at 14,000 RPM for 30 min. An aliquot from the supernatant was then dried at 105 °C overnight to calculate dry weight concentrations.

2.3. Cloud point (visual inspection)

Aqueous solutions of cellulose derivatives at 5 °C were sealed in test tubes, transferred to a water bath and heated to the desired temperature. The temperature was allowed to stabilize at the desired value and images were taken using a digital camera. After the first heating process, samples were allowed to cool down naturally and kept in the refrigerator for 1 h. Then, bath temperature was increased and the process was repeated.

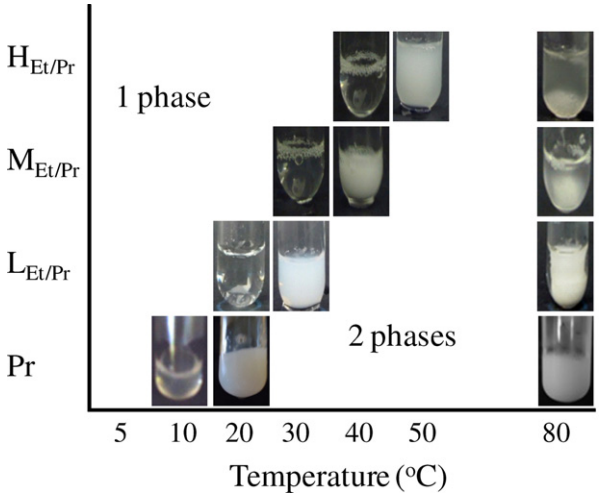

Fig. 1. Visual inspection of cloud point.

2.4. Micro-differential scanning calorimetry

Thermal characteristics of cellulose ether solutions were determined using SETARAM micro DSC-III calorimeter (Caluire, France). About 850 mg of each sample solution, with distilled water as a reference, were sealed into DSC cells. The water is required in certain amount to match the heat capacity of the sample. Both the sample and reference cells were allowed to equilibrate at 10 °C for 1 h. Temperature was then raised from 10 to either 78 or 110 °C at heating rate of 1 °C/min and then lowered immediately to 10 °C at the same rate. In case of solution of 3-*O*-propyl cellulose the starting temperature was lowered to 1 °C, to take into consideration the low temperature of the endothermic transition. Enthalpy values (ΔH), onset temperature T_o, peak temperature T_m and end temperature T_e the transition were calculated using Setaram software with an interpolated baseline.

2.5. Rheology

Dynamic viscoelastic measurements were carried out on a controlled stress rheometer (MCR 301; Anton Paar, Austria). A 25 mm diameter parallel plate geometry and 1 mm as gap were used. All measurements were performed under oscillatory shear mode at an angular frequency of 10 rad/s and a shear strain ensuring operation within the linear viscoelastic region. To prevent dehydration during the measurements a thin layer of low viscosity silicone oil was placed on the periphery surface of the solution. Elastic modulus and loss modulus were monitored employing the same heating rate (1 °C/min) and temperature ranges as for the differential scanning calorimeter experiment.

3. Results and discussion

3.1. Phase separation (visual inspection)

Fig. 1 shows changes in turbidity (visual inspection) for each of the 3-*O*-alkyl cellulose ethers equilibrated at the respective temperatures. The turbidity increases dramatically as the temperature of the solution exceeds the critical onset value, i.e. the cloud point temperature.

The dramatic increase in turbidity indicates the formation of large scale fluctuation of concentration in the system, i.e. polymer-rich and polymer lean phase. The evaluation of cloud point in this way is rather approximate, which reflects the nature of the experiment, but nevertheless it provides supportive valid information for comparison among samples. Cloud point temperature is mainly influenced by the two hydrophobic moieties present on the cellulose backbone. The lowest onset of clouding was observed for sample Pr (3-*O*-propyl cellulose) and it shifts to higher temperature as some of the propyl is replaced with ethyl groups. Thus a specific trend was observed: $Pr < L_{Et/Pr} < M_{Et/Pr} < H_{Et/Pr}$. At temperature ≥80 °C phase separation becomes more severe and formation of a "white" precipitate and a clear supernatant is observed. Interestingly sample Pr does not show any visible sign of precipitation, which seems to be promoted by high ratio of DS_{Et}/DS_{Pr}. This observation tends to suggest that the precipitation is arrested by the incipient gelation whereby "stronger" gels are produced with propyl substituent than "weaker" phase separating samples as the amount of ethyl substitution replace propyl group. Rheological measurements support this finding.

3.2. Thermally induced hydrophobic aggregation

Differential scanning calorimetry (DSC) has been used to detect thermally induced transitions in aqueous solutions of cellulose ethers, on heating and cooling at a scan rate of 1 °C/min (Fig. 2). On heating, all samples show a single broad asymmetric endothermic peak. The origin of signal in the calorimeter is believed to come from the loss of the water of hydration, which has a hydrogen-bonded structure (ice-like), and therefore the braking of such bonds requires energy input (Takahashi & Shimazaki, 2001). The onset of the endothermic trace closely matches the cloud point temperature for each sample (Fig. 1 to be compared with Fig. 2), as found for 3-*O*-ethyl cellulose (Sun et al., 2009). However the shape of the endothermic curves, which does reveal the nature of the transition, is indicative of an aggregation type of phenomena. Armstrong et al. (1995), in their study on synthetic polymers, concluded that both phase separation and aggregation give rise to an asymmetric calorimetric signal. However phase separation is characterized by a much steeper leading edge than aggregation and a "long gently sloping post transitional tail", with an enthalpy value generally smaller than the one observed for aggregation. Similar findings have been reported by Haque et al. (1993) for phase separation of fully substituted hydroxypropylcellulose ethers (DS ∼ 2.7). On cooling a single exothermic peak was also observed (Fig. 2). The similarity of the signals, heating and cooling, for sample $L_{Et/Pr}$, $M_{Et/Pr}$ and $H_{Et/Pr}$, suggests that the process occurring on cooling is the reverse of the one occurring on heating, and therefore it involves disassociation and re-hydration of the molecules (solvation) as the temperature is lowered (Fig. 2b–d). The hydration of the molecules with consequent structuring of water molecules is an exothermic event. The two signals, for sample $L_{Et/Pr}$, $M_{Et/Pr}$ and $H_{Et/Pr}$, also carry comparable calorimetric enthalpies, which indicates the almost total reversibility of the process (Table 2). Analogous comparison for sample Pr. rather difficult because part of the exotherm takes place outside the temperature range window of the experiment due to the evident hysteresis. Hysteresis, by means of difference in aggregation (heating) and disassociation (cooling) temperature (T_m) was negligible for sample $L_{Et/Pr}$ and $M_{Et/Pr}$ and it becomes noticeable for samples containing high level of propyl moiety ($Pr < H_{Et/Pr}$) Hysteresis is quite common in polysaccharide solutions, where it is associated with additional stabilization of the network (Morris, Rees, & Robinson, 1980; Rochas & Rinaudo, 1984). A similar explanation holds for sample Pr, here hysteresis might involve "strengthening", as a function of temperature, of the hydrophobic junctions between polymer chains, which allows binding between nearby sites (backbone–backbone interaction). A second cycle (heating and cooling), using the same sample, was performed with a maximum heating temperature fixed at 110 °C (Fig. 2a). On heating, above the "main" endothermic transition, and starting from 50 °C, the heat flux function changes in curvature which is a sign of different

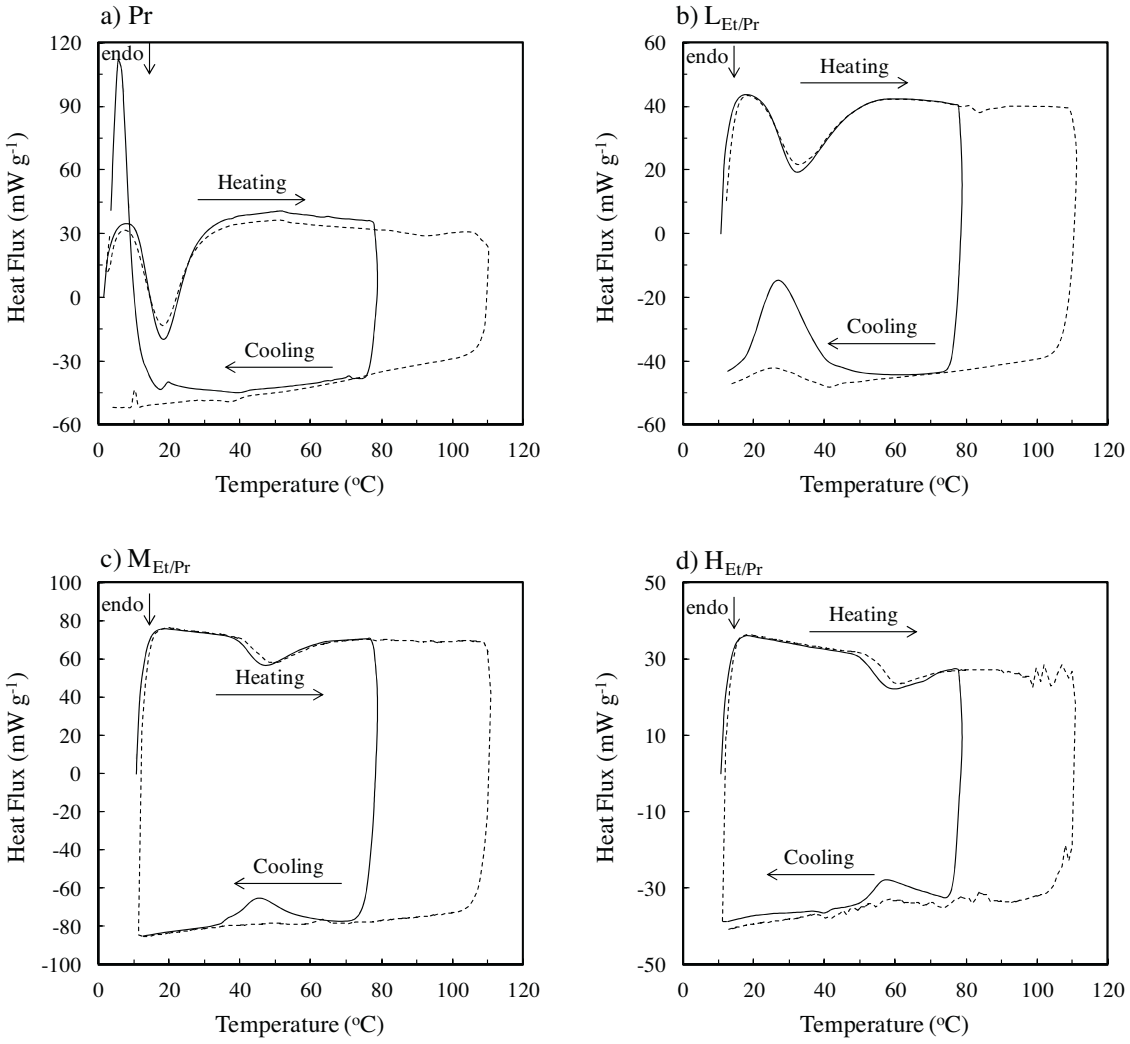

Fig. 2. Differential scanning calorimetry thermograms: (a) Pr (3-*O*-propyl cellulose), (b) $L_{Et/Pr}$ (DS_{Et} = 0.27; DS_{Pr} = 0.56), (c) $M_{Et/Pr}$ (DS_{Et} = 0.77; DS_{Pr} = 0.27) and (d) $H_{Et/Pr}$ (DS_{Et} = 0.94; DS_{Pr} = 0.15). First scanning to 78 °C (solid line) and second scanning to 110 °C (dotted line).

way the sample absorbs heat (different heat capacity) and consequently of the additional stabilization process. Heating to 110 °C is approximately 60 °C above the end of the main transition and allows the stabilization to approach completion, which either suppresses the reversible transition or shifts it to temperature much lower than 1 °C. It would be expected that if the sample Pr was to have been heated to temperatures slightly above the end of the main transition, then much less hysteresis would occur. The absence of any sign of hysteresis for both sample $H_{Et/Pr}$ and $M_{Et/Pr}$, where heating to 80 °C is close to the end of the main endothermic peak, favours this hypothesis (Fig. 2c and d). Moreover the irreversibility of the transition was seen for all the other samples when heated to 110 °C (Fig. 2b–d). On the basis of those evidences we suggest that there is a "critical temperature" above which association becomes irreversible and this temperature is a function of the ratio of the two alkyl moieties: the higher the propyl content the lower the "critical temperature". Characteristic parameters for the transitions of each of the samples studied on heating and cooling are summarized in Table 2. The enthalpy of transition, estimated from the area under the peak, is directly proportional to the level of propyl group: Pr > $L_{Et/Pr}$ > $M_{Et/Pr}$ > $H_{Et/Pr}$. The present results may reflect the different hydrophobicity of each sample. Assuming the molecular size of the two alkyl moieties is directly proportional to their "hydrophobicity" (propyl > ethyl), then the most hydrophobic sample, Pr, would aggregate first (Privalov & Gill, 1989). Moreover data reported by Sun et al. (2009) for 3-*O*-ethyl cellulose (Et) are not in line with the observed trends. In contrast to what is expected, the value reported for the enthalpy of aggregation was higher than sample $H_{Et/Pr}$. This observation suggests that the increase in enthalpy when ethyl is replaced by propyl

Table 2
Transitions parameters for regioselective substituted cellulose ethers. T_o = onset temperature; T_m = peak temperature; T_e = end set temperature and ΔH_{cal} = enthalpy of the transition.

Sample	T_o	T_m	T_{end}	ΔH (J/g solid)[b]
Heating				
Et[a]	51.0	62.0	85.0	14.7
$H_{Et/Pr}$	51.5	58.9	72.3	6.7
$M_{Et/Pr}$	39.1	47.0	61.1	11.6
$L_{Et/Pr}$	22.8	32.1	50.1	21.8
Pr	10.1	18.4	28.3	36.8
Cooling				
Et[a]				
P1	31.0	24.0	18.0	−3.4
P2	78.0	58.0	50.0	−11.3
$H_{Et/Pr}$	64.3	57.1	51.5	−5.1
$M_{Et/Pr}$	57.9	45.3	34.8	−10.9
$L_{Et/Pr}$	40.4	26.8	18.1	−22.7
Pr	19.9	9.8	n.a.	n.a.

[a] Sun et al. (2009). On cooling two separated processes were observed: P1 and P2.
[b] Enthalpy refers to gram of solute.

group cannot be explained only in terms of the "additive effect" due to the higher hydrophobicity of propyl, compared to ethyl, but additional distinctive structural characteristics come into play. In fact one should consider that regioselective substitution at position 3 does not prohibit allocation of the same moiety on adjacent anhydroglucose units, which gives rise to "blockiness". Although no data with reference to blockiness are available, for samples where the two moieties are present, it was assumed on statistical basis. The breath of the transition might be partially explained by polydispersity of the sample which also gives rise to a range of different hydrophobicity within the same sample, thus the more hydrophobic molecules (high level of propyl) would tend to aggregate first. Additionally the contribution of blockiness to the breath of the transition cannot be excluded, as seen comparing sample Pr with samples containing both alkyl moieties on the cellulose chain (Fig. 2). Sun et al. (2009) observed also the separation of two peaks for the disassociation on cooling, where the peak at low temperature was attributed to the reformation of the original cellulose structure in solution, based on the Haque and Morris (1993), Haque et al. (1993) model. The original cellulose structure in solution involves, the existence of residual crystallinity due to hydrogen bonding at the unsubstituted positions 2 and 6 as shown by Kondo et al. (2008). It follows that the presence of propyl groups, because of its molecular size, might sterically prohibit hydrogen bonding between unsubstituted carbon, which is observed as reduction of the ordering from X-ray diffraction (data not shown) and therefore suppresses the lower exothermic peak of the $H_{Et/Pr}$, $M_{Et/Pr}$ and $L_{Et/Pr}$ samples.

3.2.1. Quantitative analysis of the calorimetric data

Quantitative analysis of the calorimetric data for the aggregation process is based on a two state equilibrium model (Armstrong et al., 1995; Paterson et al., 1997):

$$nX \leftrightarrow X_n \tag{1}$$

where X represents cellulose ether unimers in solution, n the aggregation number and X_n is cellulose ethers aggregate. As a pre-requisite, the applicability of the model requires rigorous equilibrium condition throughout the temperature range (Marky & Breslauer, 1987; Sturtevant, 1982). The negligible hysteresis on cooling and the almost mirror image of the exotherm and endotherm, in the case of sample $H_{Et/Pr}$, constitute the arguments which satisfy the equilibrium condition (Fig. 2c and d). Deviations from this behaviour, as seen for sample Pr, are due to the stabilization process occurring at high temperature as argued before. The equilibrium constant for the aggregation process can be described in term of the fraction of the unimers in the aggregated state, if we define, α, the extent of aggregation as:

$$\alpha = \frac{\Delta H_T}{\Delta H_{cal}} \tag{2}$$

where ΔH_T is the accumulative heat of reaction up to a given temperature T during the aggregation process and ΔH_{cal} is the ultimate heat released during a complete reaction. Hence the equilibrium constant for the aggregation process is:

$$K = \frac{[X_n]}{[X]^n} = \frac{\alpha(C/n)}{[(1-\alpha)C]^n} \tag{3}$$

The expression of K in terms of α enables the study of the temperature dependence of K which is described by the van't Hoff equation:

$$\Delta H_{vH} = RT^2 \left[\frac{d \ln K}{dT}\right] \tag{4}$$

Table 3
Thermodynamic model parameters for 3-*O*-ethyl-propyl cellulose ethers.

Sample	n	ΔH_{vH}(J/mol^{-1})	ΔH_{cal}(J/mol^{-1})	ΔC_p (J g^{-1} K^{-1})
$H_{Et/Pr}$	2.4	410	100	−0.03
$M_{Et/Pr}$	2.8	435	188	−0.26
$L_{Et/Pr}$	3	354	327	−0.45
Pr	4	602	563	−0.53

Data from the calorimeter are converted into apparent excess heat capacity using the following formula:

$$\Phi C_{p,xs} = Hsm^{-1} \tag{5}$$

where $\Phi C_{p,xs}$(J g^{-1} K^{-1}) is the apparent excess heat capacity, H(W) the heat flux, s(K h^{-1}) the scan rate and m(g) the amount of sample. Evaluation of aggregation number, n, and the van't Hoff enthalpy (ΔH_{vH}) was carried using Eqs. (6) and (7):

$$\Delta H_{vH} = \frac{2(n+1)C_{p,1/2}RT_{1/2}^2}{\Delta H_{cal}} \tag{6}$$

$$\Phi C_{p,xs} = \frac{\Delta H_{cal}\Delta H_{vH}}{RT^2}\left(\frac{1}{1/\alpha + n/(1-\alpha)}\right) \tag{7}$$

where $C_{p,1/2}$ and $T_{1/2}$ are the value of $\Phi C_{p,xs}$ and temperature when $\alpha = 0.5$. The derivation of the Eqs. (6) and (7) is given in detail elsewhere (Armstrong et al., 1995; Paterson et al., 1997). Model fitting the experimental data was done on a spread sheet by using the Newton-Raphson procedure to minimize the standard deviation between experimental and fitted data. Calculated parameters for the aggregation process are summarized in Table 3. Interestingly the aggregation number (n) varies systematically as function of the amount of the two alkyl moieties. The higher the level of propyl the higher the aggregation number: Pr > $H_{Et/Pr}$ > $M_{Et/Pr}$ > $L_{Et/Pr}$. All samples show a value of ΔH_{vH} higher than ΔH_{cal} which is indicative of a cooperative phenomenon. The transition observed in the calorimeter can be regarded as aggregation of cooperative units (pre-aggregate) rather than single molecules. Therefore the aggregation number corresponds to the number of clusters interconnecting, which are made of more than one molecule. $\Delta H_{vH}/\Delta H_{cal}$ specifies the size of the cooperative units, in other words the molecularity of the pre-aggregates, which is borne out by comparing base molar mass of the van't Hoff enthalpy to the one of the calorimetric enthalpy. As suggested by Paterson, Armstrong, Chowdhry, and Leharne (1997), the base molar mass in ΔH_{cal} refers to moles of substance while in the van't Hoff equation the molar mass is assigned by the gas constant (C_p and the ΔH_{cal} cancel out). Negative values of ΔC_p indicate that the heat capacity of the aggregates is lower than the non aggregated molecules. Privalov and Gill (1989) reported an increase in heat capacity when a non-polar compound is dissolved in water and this increase is proportional to the surface area of the non-polar compound. Protein unfolding, likewise, is also accompanied by an increase in heat capacity due to hydration of the exposed non polar group. Hence a decrease in heat capacity accounts for the reduction of the exposure to the water trough hydrophobic association. It follows that the extent of hydrophobic association increases as function of the propyl group as observed by a decrease in ΔC_p.

3.3. Gelation

Small deformation dynamic viscoelastic measurements have been used to monitor structural changes which accompany the thermally induced aggregation of cellulose ethers in water. The concentration of each cellulose ether (6.2 wt%) and the heating rate (1 °C/min) were the same as used in the calorimetric experiment. Fig. 3a shows changes of elastic (G') modulus, loss (G'') modulus

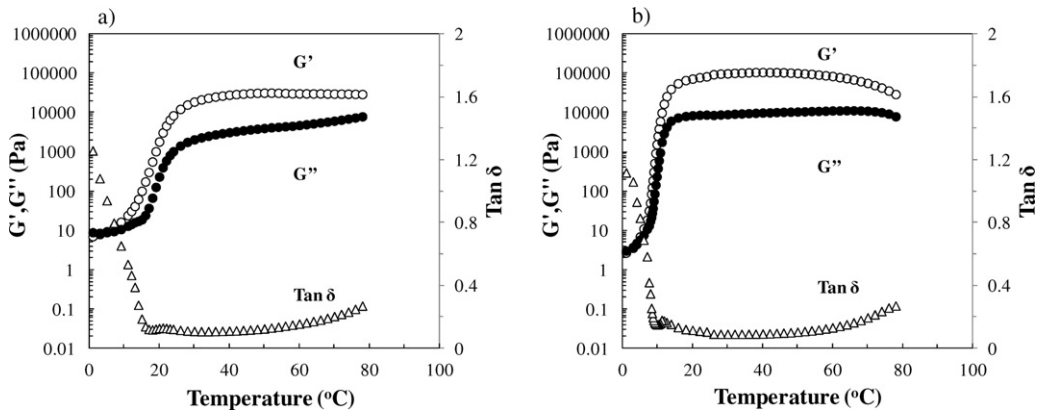

Fig. 3. Temperature sweep measurement for 3-*O*-propyl cellulose (Pr): (a) heating and (b) cooling.

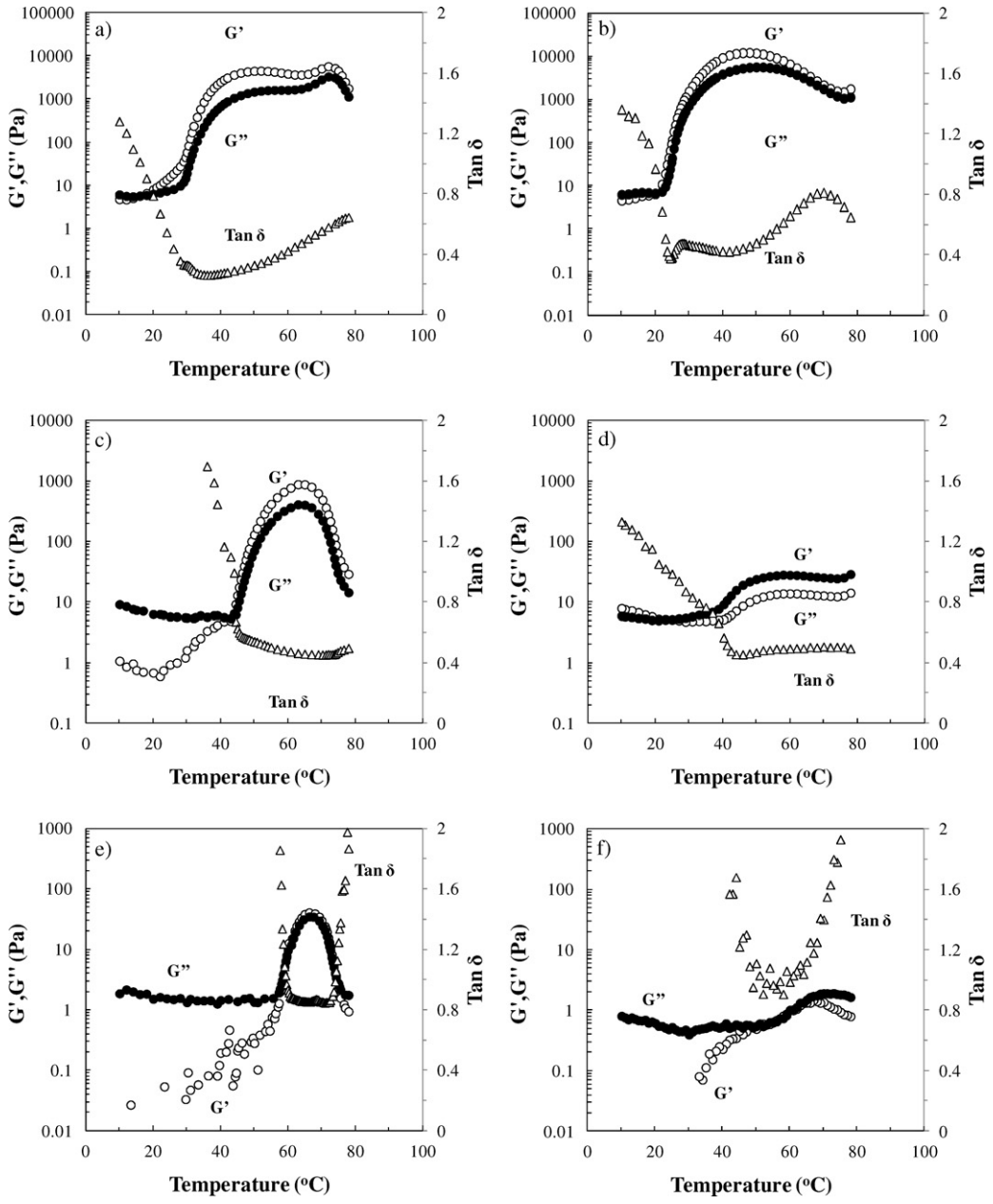

Fig. 4. Temperature sweep measurement for 3-*O*-ethyl propyl cellulose. $L_{Et/Pr}$: (a) heating and (b) cooling. $M_{Et/Pr}$: (c) heating and (d) cooling. $H_{Et/Pr}$: (e) heating and (f) cooling.

and tan δ (G''/G'), on heating, for sample Pr. At low temperature ($\sim$1 °C) the rheological properties are typical of a solution with the elastic modulus less than the viscous modulus (G''/G'). The structural changes occur in a two step fashion, previously reported for other cellulose ethers (Desbrieres et al., 1998; Haque & Morris, 1993; Hirrien et al., 1996). As the temperature increases, G' firstly increases smoothly until 10 °C (onset of the second step) from which it changes more rapidly with temperature. The crossover of the moduli, which marks the boundary between liquid and solid like behaviour, occurs at temperature of about 5 °C. However, the cross over occurs in the range of temperature which is calorimetrically silent therefore it is not related with the hydrophobic aggregation. Consequently the onset of the second G' increase, which closely matches the onset of the endotherm, is more likely to correspond to the T_{gel}. This assertion is corroborated by the fact that the correspondence between T_o and onset of the second step of G'' increase was observed for all samples studied. On further heating, above 50 °C, G' attains a plateau with a magnitude of 30 kPa. G'' changes with similar profile, however it does not level off at high temperature but it shows, instead, a steady increase. According to the rubber theory, the elasticity of the gel-network is intimately related to the number of elastic active chains which are the chains between two cross-link junctions. This number stays constant at temperature above 50 °C as indicated by G' plateau, which suggests that the structural stabilization, observed in the calorimeter as changes in heat flux curvature above 50 °C (Fig. 2a), does not involve formation of any additional junction zones but instead it is associated with changes in loss modulus. Additionally as pointed out in the previous section, aggregation can be regarded as clusters interconnecting at high temperature ($\Delta H_{vH}/\Delta H_{cal} > 0$). Aggregation among clusters is observed as an increase, in G', on the other hand the growth of each cluster, which do not contribute to the formation of junction zone (or elastic active chains) accounts for G'' increase and heat capacity changes. On cooling the gel-network reverts to a solution as shown in Fig. 3b. Interestingly the magnitude of both moduli at the beginning of the cooling is higher than the magnitude at comparable temperature on heating. The structural stabilization occurs at high temperature and as the samples are cooled the junctions formed become thermodynamically unstable, additionally the increase in modulus might reflect the start of irreversibility seen at temperature above 80 °C. From the plateau region the two moduli sharply fall to almost their original value, confirming the gelation process is reversible. Comparison between the onset of network formation on heating and the onset of the network collapse on cooling confirms the hysteresis observed in the calorimeter. The replacement of some propyl with ethyl group causes changes in the gelation properties as expected. Fig. 4a shows structural changes on heating for sample $L_{Et/Pr}$. Both moduli increase with a similar shape seen per sample Pr. The main differences are: the temperature at which the major changes occur and the magnitude of both moduli. The onset of the second dramatic increase is close to 30 °C almost 20 °C higher than for Pr, confirming the trend observed in the calorimetric experiment: the substitution of the ethyl group increases the transition temperature. The maximum value reached by G' is one order of magnitude lower than Pr. The presence of a maxima for both moduli is a consequence of the beginning of the macroscopic phase separation occurring at high temperatures which is a result of heterogeneity of the sample between the two plates in the rheometer. Indeed separation into a polymer rich and polymer poor phase is what was observed visually in the test tube at high temperature (Fig. 1). However on cooling (Fig. 4b) a sign of reversibility is still observed, mirrored also by an increase in both moduli upon cooling which then revert to their original value with a much less prominent hysteresis than sample Pr. sample $M_{Et/Pr}$ on heating is shown in Fig. 4c. The same consideration on the structural development can be made for this sample. The initial decrease of both moduli upon heating to a temperature of about 20 °C, is more evident than both sample Pr and $L_{Et/Pr}$, as expected for a homogeneous polymer solution (Williams, 1975). However above 20 °C a two step increase in G' is seen, consistent with the previous samples, only at a higher temperature, and with what has been reported previously (Haque & Morris, 1993; Haque et al., 1993). The decrease of the two moduli upon further heating is more evident than sample $L_{Et/Pr}$ as consequence of the more severe macro-phase separation observed visually for this sample (Fig. 1) and occurs on cessation of the endotherm signal (Fig. 2). Hysteresis on cooling was negligible (Fig. 4d), matching the calorimetric result. Rheologically, the same trends are seen with a further increase in ethyl content (Fig. 4e and f), with an increase in temperature required for gelation, a lower modulus (elastic) of the gel formed and an increase in the catastrophic collapse of the structure, again coinciding with the end of the endotherm. Initial values of G' are too low to be measured and start to be detected when temperatures approach 40 °C. The onset of the second dramatic increase in modulus is around 56 °C the highest among the samples studied. Above 56 °C the two moduli steeply increase although G' never considerably exceeds G'', which, in the absence of a frequency sweep measurement, is an indication of a weak gel. The general observation from these experiments is that on increase in the amount of a more hydrophobic moiety (Pr) increases the elastic modulus and the network is also more coherent with a steady decrease in tan δ as Pr increases.

4. Conclusion

The thermally induced aggregation of new regioselective substituted 3-*O*-ethyl-propyl cellulose ethers in water has been described with reference to aggregation of clusters, rather than single molecules, which interconnect forming an opaque gel network as the temperature increases. The ratio of the two alkyl moieties on to the cellulose chain has great influence on the number and structure of aggregates, and on the temperature of the transition and as consequence on the mechanical characteristic of the gel. The discussion, explaining how the ratio of the two hydrophobic moieties determines the aggregation process and the characteristic of the aggregates, is based on the central argument that hydrophobicity underpins the aggregation. As ethyl is replaced by propyl group the material becomes more hydrophobic and the aggregation temperature decreases. This is due to the undesirable entropy decrease of water surrounding the hydrophobic moieties which is proportional to the size of the hydrophobic moieties (Privalov & Gill, 1989). It follows that the cellulose ethers containing a high level of propyl moieties (more hydrophobic) are associated to a high entropic penalty, which outweigh the enthalpy term at lower temperature than the cellulose containing less propyl (less hydrophobic). Overall we concluded that the more hydrophobic the cellulose ether, the higher the aggregation number (n) (more aggregates coming together) and the "stronger" the gel. However, in addition to the hydrophobicity, it is tentatively suggested that the presence of the two moieties give rise to blockiness which also has to be considered to fully explain the physico-mechanical properties of the material. This suggestion is based on the scientific evidence provided by Williams, Foster, and Schols (2003) and Ström et al. (2007) in regard to the presence of blockiness and its effect on the rheological properties of pectin gels. Comparison with the work of Sun et al. (2009), on 3-*O*-ethyl cellulose (Et), suggests that the increase in enthalpy when ethyl is replaced by propyl group cannot be explained only in terms of the "additive effect" due to the higher hydrophobicity of propyl, compared to ethyl, but additional distinctive structural characteristics come into play. Since both alkyl groups are capable of interaction, a question

would be: Which moiety is involved in the junctions? Are the junctions made of both propyl and ethyl? As a starting point, it is worth clarifying the meaning of "mixed junctions". The two moieties on different cellulose ethers molecules might either interact with partners of different kind (propyl–ethyl) or with partner of the same kind (propyl–propyl; ethyl–ethyl). The argument against the former type of interaction is based on the theory of "like likes like", thus each moiety will prefer to face moiety of the same kind (lower energy). The later type of interaction would assume the co-existence of both propyl–propyl and ethyl–ethyl on the same molecule. This would be highly improbable due to steric reasons. In other words, it would be difficult for a junction zone made of ethyl group to accommodate the adjacent propyl group due to different molecular size. Therefore, a hypothesis is that in the case of 3-*O*-ethyl propyl the junction zone are made of propyl groups and interrupted by the presence of the ethyl groups. The ethyl–ethyl interaction occurs only in the case of 3-*O*-ethyl cellulose (Sun et al., 2009), where ethyl is the only moiety present. We speculate that for 3-*O*-butyl propyl cellulose then the junction would be made of the butyl moiety for the same reason. In force of this view is the evidence that sample containing both substituents shows lower elastic modulus and transition enthalpy compared to the 'pure' propyl containing or ethyl containing samples. The aggregation is reversible as the gel reverts back to the solution state on cooling. However reversibility persists unless the solution is "overheated". In fact heating above the "main" endothermic transition resulted in a further stabilization of the gel structure. The stabilization process was ascribed to the "strengthening", as a function of temperature, of the hydrophobic junctions between polymer chains, which allows binding between neighbouring polymer backbones.

References

Armstrong, J., Chowdhry, B., O'Brien, R., Beezer, A., Mitchell, J., & Leharne, S. (1995). Scanning microcalorimetric investigations of phase transitions in dilute aqueous solutions of poly(oxypropylene). *The Journal of Physical Chemistry*, *99*(13), 4590–4598.

Chevillard, C., & Axelos, M. (1997). Phase separation of aqueous solution of methylcellulose. *Colloid & Polymer Science*, *275*(6), 537–545.

Desbrieres, J., Hirrien, M., & Rinaudo, M. (1998). Relation between the conditions of modification and the properties of cellulose derivatives: Thermogelation of methylcellulose. In T. J. Heinze, & W. G. Glasser (Eds.), *Cellulose derivatives* (pp. 332–348). Washington: American Chemical Society.

Desbrières, J., Hirrien, M., & Ross-Murphy, S. B. (2000). Thermogelation of methylcellulose: Rheological considerations. *Polymer*, *41*(7), 2451–2461.

Funami, T., Kataoka, Y., Hiroe, M., Asai, I., Takahashi, R., & Nishinari, K. (2007). Thermal aggregation of methylcellulose with different molecular weights. *Food Hydrocolloids*, *21*(1), 46–58.

Fox, S. C., Li, B., Xu, D., & Edgar, K. J. (2011). Regioselective esterification and etherification of cellulose: A review. *Biomacromolecules*, *12*(6), 1956–1972.

Ganz, A. J. (1977). Cellulose hydrocolloids. In H. Graham (Ed.), *Food colloids* (pp. 382–417). Westport, CT: AVI Press.

Grover, J. S. (1993). Methyl cellulose and its derivatives. In R. L. Whistler, & J. N. BeMiller (Eds.), *Industrial gums: Polysaccharides and derivatives* (3rd ed., pp. 475–504). London: Academic Press.

Haque, A., & Morris, E. R. (1993). Thermogelation of methylcellulose. Part I: Molecular structures and processes. *Carbohydrate Polymers*, *22*(3), 161–173.

Haque, A., Richardson, R. K., Morris, E. R., Gidley, M. J., & Caswell, D. C. (1993). Thermogelation of methylcellulose. Part II: Effect of hydroxypropyl substituents. *Carbohydrate Polymers*, *22*(3), 175–186.

Heinze, T., & Petzold, K. (2008). Cellulose chemistry: Novel products and synthesis paths. In B. Mohamed Naceur, & G. Alessandro (Eds.), *Monomers, polymers and composites from renewable resources* (pp. 343–368). Amsterdam: Elsevier.

Heinze, T., Pfeifer, A., Sarbova, V., & Koschella, A. (2011). 3-O-propyl cellulose: Cellulose ether with exceptionally low flocculation temperature. *Polymer Bulletin*, *66*(9), 1219–1229.

Heinze, T., Wang, Y., Koschella, A., Sullo, A., & Foster, T. J. (2012). Mixed 3-mono-O-alkyl cellulose: Synthesis, structure characterization and thermal properties. *Carbohydrate Polymers*, *90*, 380–386.

Heymann, E. (1935). Studies on sol–gel transformations. I. The inverse sol–gel transformations of methylcellulose in water. *Trans Faraday Society*, *31*, 846–863.

Hirrien, M., Chevillard, C., Desbrières, J., Axelos, M. A. V., & Rinaudo, M. (1998). Thermogelation of methylcellulose: New evidence for understanding the gelation mechanism. *Polymer*, *39*(25), 6251–6259.

Hirrien, M., Desbrières, J., & Rinaudo, M. (1996). Physical properties of methylcellulose in relation with the conditions for cellulose modification. *Carbohydrate Polymers*, *31*(4), 243–252.

Ibbett, R. N., Philp, K., & Price, D. M. (1992). 13C n.m.r. studies of the thermal behaviour of aqueous solutions of cellulose ethers. *Polymer*, *33*(19), 4087–4094.

Israelachvili, J., & Pashley, R. (1982). The hydrophobic interaction is long range, decaying exponentially with distance. *Nature*, *300*(5890), 341–342.

Kato, T., Yokoyama, M., & Takahashi, A. (1978). Melting temperatures of thermally reversible gels IV. Methyl cellulose–water gels. *Colloid & Polymer Science*, *256*(1), 15–21.

Kobayashi, K., Huang, C.-i., & Lodge, T. P. (1999). Thermoreversible gelation of aqueous methylcellulose solutions. *Macromolecules*, *32*(21), 7070–7077.

Kondo, T., Koschella, A., Heublein, B., Klemm, D., & Heinze, T. (2008). Hydrogen bond formation in regioselectively functionalized 3-mono-O-methyl cellulose. *Carbohydrate Research*, *343*(15), 2600–2604.

Koschella, A., Fenn, D., Illy, N., & Heinze, T. (2006). Regioselectively functionalized cellulose derivatives: A mini review. *Macromolecular Symposia*, *244*(1), 59–73.

Li, L. (2002). Thermal gelation of methylcellulose in water: Scaling and thermoreversibility. *Macromolecules*, *35*(15), 5990–5998.

Li, L., Thangamathesvaran, P. M., Yue, C. Y., Tam, K. C., Hu, X., & Lam, Y. C. (2001). Gel network structure of methylcellulose in water. *Langmuir*, *17*(26), 8062–8068.

Marky, L. A., & Breslauer, K. J. (1987). Calculating thermodynamic data for transitions of any molecularity from equilibrium melting curves. *Biopolymers*, *26*(9), 1601–1620.

Morris, E. R., Rees, D. A., & Robinson, G. (1980). Cation-specific aggregation of carrageenan helices: Domain model of polymer gel structure. *Journal of Molecular Biology*, *138*, 349–362.

Nishinari, K., Hofmann, K. E., Moritaka, H., Kohyama, K., & Nishinari, N. (1997). Gel–sol transition of methylcellulose. *Macromolecular Chemistry and Physics*, *198*(4), 1217–1226.

Paterson, I., Armstrong, J., Chowdhry, B., & Leharne, S. (1997). Thermodynamic model fitting of the calorimetric output obtained for aqueous solutions of oxyethylene–oxypropylene–oxyethylene triblock copolymers. *Langmuir*, *13*(8), 2219–2226.

Privalov, P. I., & Gill, S. J. (1989). The hydrophobic effect: Are appraisal. *Pure and Applied Chemistry*, *61*(6), 1097–1104.

Robitaille, L., Turcotte, N., Fortin, S., & Charlet, G. (1991). Calorimetric study of aqueous solutions of hydroxypropyl cellulose. *Macromolecules*, *24*(9), 2413–2418.

Rochas, C., & Rinaudo, M. (1984). Mechanism of gel formation in κ-carrageenan. *Biopolymers*, *23*(4), 735–745.

Sarkar, N. (1979). Thermal gelation properties of methyl and hydroxypropyl methylcellulose. *Journal of Applied Polymer Science*, *24*(4), 1073–1087.

Sarkar, N. (1995). Kinetics of thermal gelation of methylcellulose and hydroxypropylmethylcellulose in aqueous solutions. *Carbohydrate Polymers*, *26*(3), 195–203.

Sarkar, N., & Walker, L. C. (1995). Hydration–dehydration properties of methylcellulose and hydroxypropylmethylcellulose. *Carbohydrate Polymers*, *27*(3), 177–185.

Ström, A., Ribelles, P., Lundin, L., Norton, I., Morris, E. R., & Williams, M. A. K. (2007). Influence of pectin fine structure on the mechanical properties of calcium–pectin and acid–pectin gels. *Biomacromolecules*, *8*(9), 2668–2674.

Sturtevant, J. M. (1982). A scanning calorimetric study of small molecule–lipid bilayer mixtures. *Biochemistry*, *79*, 3963–3967.

Sun, S., Foster, T. J., MacNaughtan, W., Mitchell, J. R., Fenn, D., Koschella, A., et al. (2009). Self-association of cellulose ethers with random and regioselective distribution of substitution. *Journal of Polymer Science Part B: Polymer Physics*, *47*(18), 1743–1752.

Takahashi, M., & Shimazaki, M. (2001). Formation of junction zones in thermoreversible methylcellulose gels. *Journal of Polymer Science Part B: Polymer Physics*, *39*(9), 943–946.

Tanford, C. (1978). The hydrophobic effect and the organization of living matter. *Science*, *200*(4345), 1012–1018.

Wiggins, P. M. (1997). Hydrophobic hydration, hydrophobic forces and protein folding. *Physica A: Statistical Mechanics and its Applications*, *238*(1–4), 113–128.

Williams, M. A. K., Foster, T. J., & Schols, H. A. (2003). Elucidation of pectin methylester distributions by capillary electrophoresis. *Journal of Agricultural and Food Chemistry*, *51*(7), 1777–1781.

Williams, M. C. (1975). Molecular rheology of polymer solutions: Interpretation and utility. *AIChE Journal*, *21*(1), 1–25.

Yaminsky, V. V., & Erwin, A. V. (2001). Hydrophobic hydration. *Current Opinion in Colloid & Interface Science*, *6*, 342–349.